Theoretical Light-Scattering Power of TiO_2 and Microvoids

William D. Ross

E. I. du Pont de Nemours & Co., Pigments Department, Experimental Station, Wilmington, Delaware 19898

The theoretical maximum light-scattering power of bubbles at low concentration in resin is 12% of that of rutile. A layer of foamed resin having 50% voids, with ideal structure, might have half the scattering power of a layer of TiO_2 enamel of equal thickness. Foam of much lower density might have twice this for equal solid content. Orienting the internal structure to parallel the surface could triple this. TiO_2 dispersed in foam might have twice to fourfold the scattering of TiO_2 in resin. Reflection at the inside of the surface of the layer is important in this comparison.

Introduction

This paper estimates how well an ideal microporous white coating might compare with a conventional white paint with respect to light-scattering power. It discusses the scattering power of rutile titanium dioxide dispersed in resin and in air, of bubbles in resin, of foams, and of TiO_2 in foams.

Light Scattering by TiO_2

How an isolated sphere scatters can be calculated by Mie theory (Mie, 1908; van de Hulst, 1957; Kerker, 1969). It depends on the refractive index and diameter of the particle, the refractive index of the surrounding medium, and the wavelength of the light. All values herein will be for wavelength 560 nm. Refractive index 1.514 is used for resin.

Most of the light which enters a film of white paint is scattered many times before escaping back into the air. We are interested in the ability of the pigment to reflect light, which is measured by the scattering coefficient, S, of Kubelka and Munk (1931) (also Kubelka, 1948). Theoretically, for particles of uniform diameter, it is proportional to the apparent scattering cross section of one particle, divided by its volume, times the mean of (1 − cosine of scattering angle), times factors which depend on the conditions of illumination and viewing (Ross, 1971).

Figure 1 shows the theoretical scattering coefficient of spheres of rutile TiO_2 in resin, as a function of diameter. The maximum is $3.36/\mu m$ of TiO_2, at diameter 0.204 μm. In an actual pigment, the particles have a distribution of size and therefore a lesser scattering coefficient.

Figure 2 shows scattering coefficients actually measured on a series of enamels made with one sample of rutile pigment, with concentrations ranging up to 35% pigment by volume (Bruehlman and Ross, 1969). The maximum scattering coefficient, at low concentrations, is $2.2/\mu m$ of TiO_2, which is two-thirds of the theoretical peak of Figure 1.

Figure 3 shows the theoretical scattering coefficient of spheres of rutile dispersed in air, as a function of diameter. The maximum, at diameter 0.205 μm, is $20.3/\mu m$ of TiO_2, or 6 times as great as for the same particles dispersed in resin. This peak is much narrower than the peak of Figure 1, so that the average for the actual particle size distribution of a pigment would be not as much as 6 times as great in air as in resin, but perhaps around 4 times as great. We do not have measurements on dispersions in air which are good enough to compare with theory.

It is essential for our later discussion to understand why scattering in air is so much greater than in resin. There are three reasons.

First, the scattering cross section, regardless of direction of scattering, is different. At the optimum diameter, 0.205 μm, the scattering cross section in air is twice that in resin, but the difference is not so great at other sizes.

Second, the angular distribution of scattered light is different. Figure 4 represents a ray of light coming from the left, in resin, and striking a spherical particle of rutile, 0.205 μm in diameter, represented by the dot in the center of the figure. The large oval is a polar graph showing the relative intensity of the scattered light as a function of angle. Nearly all the light is scattered into the forward hemisphere, and very little into the backward hemisphere.

Figure 5 is a similar graph for scattering by a rutile particle of the same size in air. Again most of the light is scattered into the forward hemisphere, but here a considerable amount is scattered into the backward hemisphere. The difference gives the particle in air an advantage of about 50% compared with the particle in resin. The comparison depends on size.

The third reason for the greater scattering in air is most important to the topic of microvoid coatings. Beneath the surface of a white enamel, scattered light travels in all directions. For resin of refractive index 1.514, all rays striking the surface more than 41° to the normal are totally reflected. At lesser angles, rays are mostly refracted into the air, but partially reflected. Of the light reaching the surface, 60% is reflected downward, where part may be absorbed. This decreases the reflectance of the pigmented layer as measured in air below that which might be measured by a photometer immersed in oil with the sample (Ryde, 1931; Saunderson, 1942). Therefore, the scattering coefficient calculated from the external measurement of reflectance is less than the internal scattering coefficient. Figure 6 shows how their ratio depends on the refractive index of the matrix (Ross, 1971). At refractive index 1.514, the ratio is 0.48.

Light Scattering by Voids

Figure 7 shows the theoretical scattering coefficient of air bubbles dispersed in resin at low concentration, as a function of diameter. The maximum is $0.401/\mu m$ at diameter 0.225 μm. This is only 12% as great as the maximum for rutile in resin.

Some writers have stated that the optimum diameter of bubbles is 0.7 μm (Kershaw, 1971). What they have calculated concerns the ratio of scattering cross section to geometrical cross section, as shown in Figure 8. Here the first peak is at 0.75 μm. This is an intermediate stage in the computation, but not the final answer, which predicts the Kubelka–Munk reflective scattering coefficient per unit volume of bubbles.

Thus, at low concentration, bubbles are relatively poor

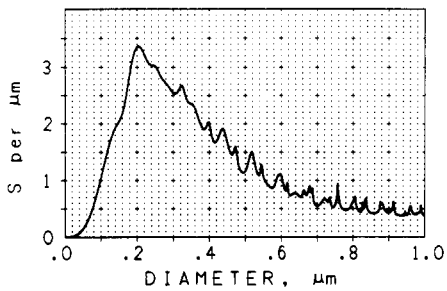

Figure 1. Theoretical Kubelka-Munk scattering coefficient of uniform spheres of rutile dispersed in resin at low concentration, as a function of diameter

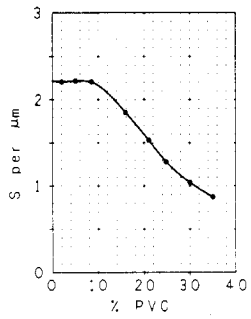

Figure 2. Measured Kubelka-Munk scattering coefficient of one sample of rutile pigment in enamel, as a function of the concentration of pigment by volume

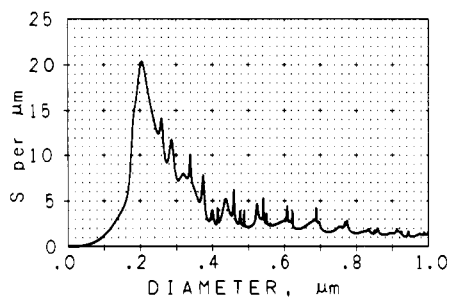

Figure 3. Theoretical Kubelka-Munk scattering coefficient of uniform spheres of rutile dispersed in the air at low concentration, as a function of diameter

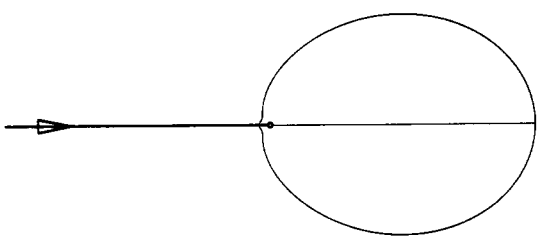

Figure 4. Polar graph of theoretical angular variation of intensity of light scattered by a rutile sphere, 0.205 μm in diameter, in resin. Light comes from the left. The scale is arbitrary

scatterers. But, if the fraction of voids is large, the picture changes. Figure 9 indicates a cross section of a foam resembling soap suds. Thin, flat walls separate bubbles. The prominent dashed line indicates a ray of light entering from above. It travels straight through the foam, but at each wall a small part is reflected, as shown by the lines of short dashes. These are in turn reflected as shown by the dotted lines. From the laws of reflection, we can calculate a Kubelka-Munk scattering coefficient, as a function of the thickness of the films between bubbles shown in Figure 10. The optimum thickness is 0.065 μm, with a scattering coefficient of 0.65/μm of resin. In such a

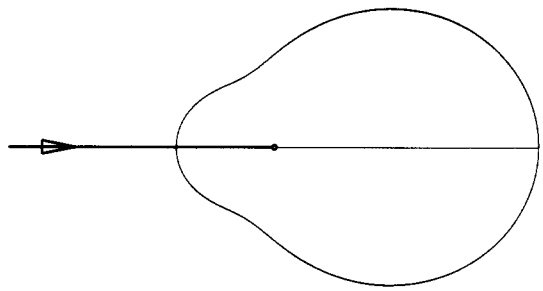

Figure 5. Polar graph of theoretical angular variation of intensity of light scattered by a rutile sphere, 0.205 μm in diameter, in air. Light comes from the left. The scale is arbitrary.

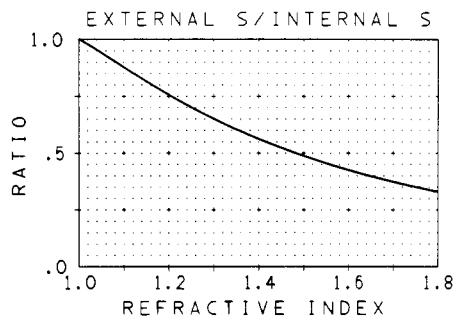

Figure 6. Theoretical effect of internal reflection at the surface of a layer of white paint. Ratio of the observable Kubelka-Munk scattering coefficient to the hypothetical coefficient beneath the surface, as a function of the refractive index of the medium in which the scattering pigment is dispersed

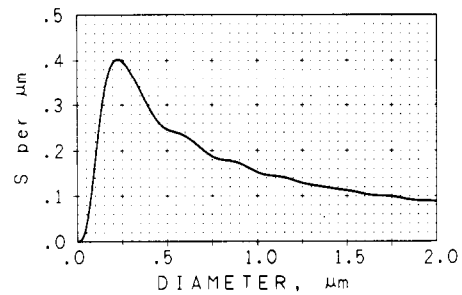

Figure 7. Theoretical Kubelka-Munk scattering coefficient of uniform spherical bubbles in resin at low concentration, as a function of diameter

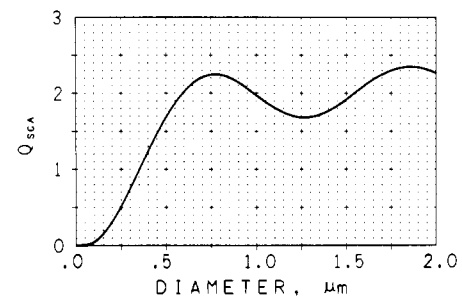

Figure 8. Theoretical ratio of total scattering cross section to geometrical cross section of uniform spherical bubbles in resin at low concentration, as a function of diameter

foam, there is no strong subsurface reflection to diminish the external diffuse reflection to less than the internal.

Some foamed plastic sheets are so formed that the walls between bubbles are mostly nearly parallel to the surface of the sheet. Such a sheet could have an additional advantage in reflecting power, of as much as a factor of 3, as shown by Figure 11.

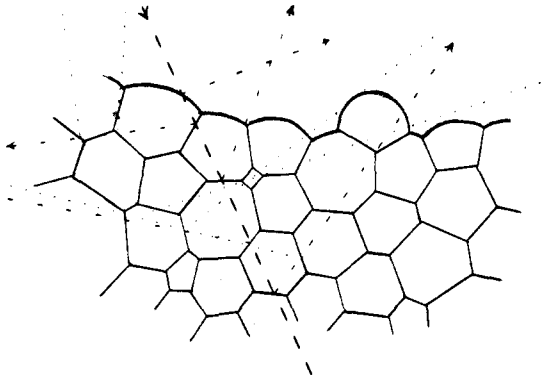

Figure 9. Idealized cross section of a foam of low density. Heavy broken line indicates a ray of light entering. Other dashed and dotted lines indicate rays reflected by the walls between bubbles

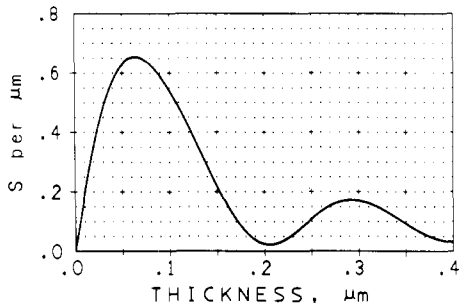

Figure 10. Theoretical Kubleka-Munk scattering coefficient, per micrometer of resin, of a foam such as illustrated in Figure 9, having walls of uniform thickness between bubbles, as a function of the thickness of these walls

The porous materials in which we are really interested have intermediate fractions of voids. We cannot rigorously calculate theoretical hiding power of such systems. Figure 12 is an attempt to interpolate between theoretical limits of the greatest possible scattering by bubbles at low concentration and by foams of low solids content. The ordinate is scattering coefficient per micrometer of thickness of coating. The two curves which are highest on the far left are for enamels pigmented with TiO_2, for comparison. The lower TiO_2 curve is based on the measurements of Figure 2. The line above it is the theoretical maximum value from Figure 1. The left end of the bottom curve shows the highest theoretical value for spherical air bubbles, from Figure 7. The right end of the bottom curve starts with the highest values for a foam as shown in Figure 10 but bends down because the loss due to internal reflection at the surface increases in proportion to solid content and is assumed to reach its full effect at 50% void. Around 50% void, the optimum structure might have polyhedral bubbles around 0.28-μm diameter, separated by walls about 0.065 μm thick. The curve shows that this could have about half the scattering coefficient of an enamel with TiO_2.

The upper line on the right is for foams in which nearly all the walls between voids are parallel to the surface and of optimum thickness but spaced at random. The line which comes up from the left, above that for spherical bubbles, is for thin discoid bubbles of optimum thickness, parallel to the surface and randomly spaced. The region between these limits might have greater scattering power than enamels with TiO_2.

Figure 13 shows the same information as Figure 12 but with the scattering coefficient reported per micrometer of solid. This may be of more interest in economic comparisons if the gas costs much less than the solid. On this basis, a foam of low density could be better than a TiO_2 enamel.

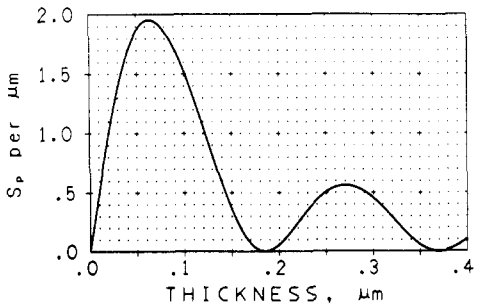

Figure 11. Theoretical Kubelka-Munk scattering coefficient, per micrometer resin, of a foam which is flattened so that the walls between bubbles are predominantly parallel to the surface, these walls being of uniform thickness, as a function of this thickness

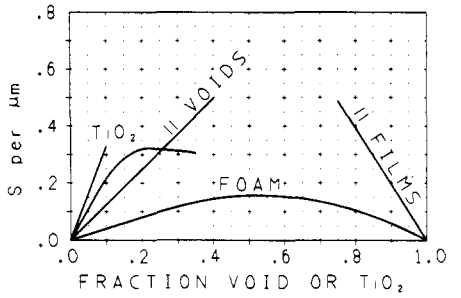

Figure 12. Theoretical ultimate Kubelka-Munk scattering coefficient per micrometer of thickness of foam layer as a function of the fraction void, compared with that of an enamel pigmented with TiO_2, as a function of TiO_2 by volume. See text for description of each curve

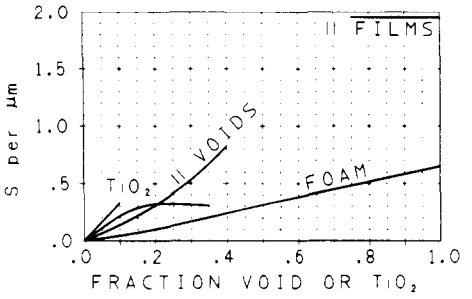

Figure 13. The same as Figure 12, except that the scattering coefficient is per micrometer of solid content of layer

TiO_2 Plus Voids

Seiner and Gerhart (1972, 1973) reported that the scattering power of TiO_2 in resin is greatly increased by the formation of voids, although similar voids in resin without TiO_2 have little scattering power. They do not give enough information for detailed analysis of the measurements.

The scattering power of TiO_2 in porous resin should be intermediate between its values in resin, Figures 1 and 2, and in air, Figure 3. The actual value will depend on the geometry of the system and cannot be described by a single formula.

Figure 14 suggests some ways in which TiO_2 might be mixed into foams. The gray background represents resin, the white circles are bubbles, and the black spots are TiO_2 particles.

In Figure 14a the bubbles are of optimum size for scat-

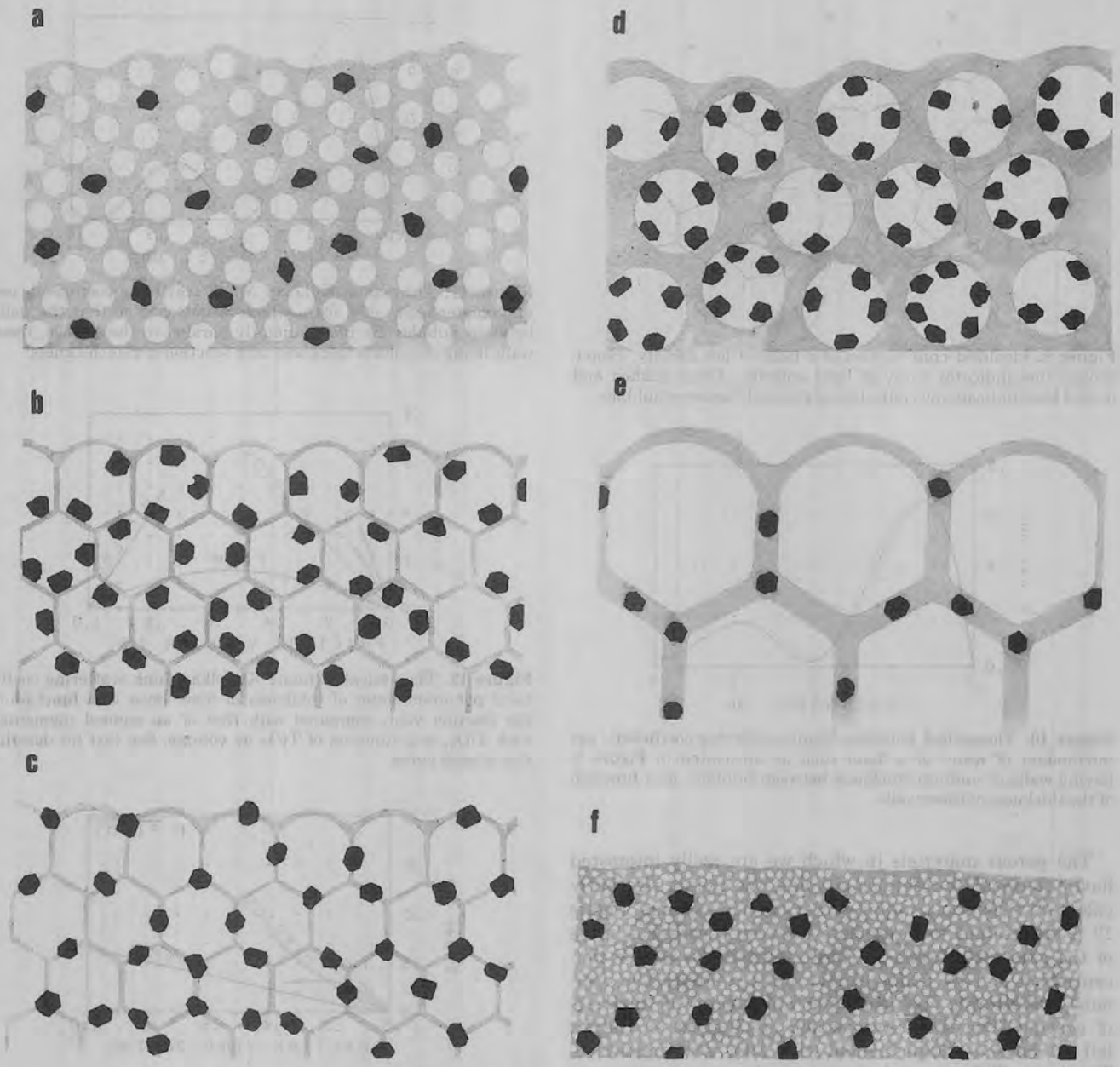

Figure 14. Idealized cross sections illustrating possible types of distributions of TiO_2 particles in foams. Black represents TiO_2, gray represents resin, and white represents air. *See text for discussion of differences*

tering, slightly larger than the TiO_2 particles. The concentration of bubbles is low enough to permit strong internal reflection at the surface. The contributions of the TiO_2 and of the bubbles should simply add, and here the proportions are drawn so that they would be about equal.

Figure 14b shows a foam having very little resin in thin walls. The bubbles are large. The TiO_2 particles are entirely in the air and are simply supported by the resin. The scattering should be that of TiO_2 dispersed in air. The resin should have very little effect. Rays of light from the TiO_2 particles should pass through the upper film of resin with very little reflection.

Figure 14c is slightly different from Figure 14b because the TiO_2 particles penetrate the resin films. Some light will be scattered into the resin films, but these are so thin that most of the light will be scattered into air. So here, too, the scattering will be mostly that of TiO_2 dispersed in air, and the resin will have only a small effect.

Figure 14d differs from the previous two because the proportion of resin is much greater. The TiO_2 particles are entirely in the air and therefore scatter strongly within the bubbles. But scattered light emerging from the bubbles and striking the surface at angles far from the vertical will be strongly reflected. This will cut the scattering coefficient to something between that of TiO_2 in air and TiO_2 in resin. The bubbles are too large to scatter strongly themselves.

Figure 14e shows much larger bubbles and TiO_2 particles entirely in the resin. But the proportion of resin is low, so that most of the scattered light will be refracted into the air. The top layer will not reflect this part of the scattered light strongly. Therefore, the scattering will be intermediate between that of TiO_2 in air and in resin.

Figure 14f shows bubbles much too small to scatter strongly and much smaller than the TiO_2 particles. In effect, the porous resin is a medium of refractive index intermediate between that of resin and of air. This affects both the scattering by the TiO_2 and the internal reflection at the surface. Therefore, the scattering will be intermediate.

Conclusion

A foam with TiO_2 ought to have at least 50% voids and closely controlled dimensions for its scattering power to begin to compete with that of an enamel pigmented with TiO_2. But TiO_2 dispersed in a foam may show scattering power intermediate between that of TiO_2 in resin and TiO_2 in air, depending on the geometry of the dispersion.

Literature Cited

Bruehlman, R. J., Ross, W. D., *J. Paint Technol.*, **41**, No. 538, 584 (1969).
Kerker, M., "The Scattering of Light and Other Electromagnetic Radiation," Chapters 3 and 4, Academic Press, New York, N. Y., 1969.
Kershaw, R. W., *Aust. Oil Colour Chem. Ass. Proc. News.* **8**, 4 (1971).
Kubelka, P., *J. Opt. Soc. Amer.*, **38**, 448 (1948).
Kubelka, P., Munk, F., *Z. Tech. Phys.*, **12**, 593 (1931).
Mie, G., *Ann. Phys. (Leipzig)*, [4] **25**, 377 (1908).
Ross, W. D., *J. Paint Technol.*, **43**, No. 563, 50 (1971).
Ryde, J. W., *Proc. Roy. Soc., Ser. A.*, **131**, 451 (1931).
Saunderson, J. L., *J. Opt. Soc. Amer.*, **32**, 727 (1942).
Seiner, J. A., Gerhart, H. L., *FATIPEC Congr.*, **11**, 127 (1972).
Seiner, J. A., Gerhart, H. L., *Ind. Eng. Chem., Prod. Res. Develop.*, **12** 98 (1973).
van de Hulst, H. C., "Light Scattering by Small Particles," Chapters 9 and 10, Wiley, New York, N. Y., 1957.

Received for review August 27, 1973
Accepted December 7, 1973

Presented at the Division of Organic Coatings and Plastics Chemistry, 166th National Meeting of the American Chemical Society, Chicago, Ill., Aug 1973.

CATALYST SECTION

Noncatalytic Gas–Solid Reaction. Chromium Oxide Catalyst in Methanol Synthesis

Roberto J. J. Williams and Roberto E. Cunningham*

Departamento de Tecnología Química, Facultad de Ciencias Exactas, Universidad Nacional de La Plata, La Plata, Argentina

The reaction pattern for the industrial process which leads to the obtention of a zinc oxide–chromium oxide catalyst for methanol synthesis is established. The process has three well-defined stages: (a) chromium trioxide reaction with an excess of zinc oxide and water leading to a mixture of zinc hydroxychromates; (b) formation of zinc oxide and zinc dichromate by heating the zinc hydroxychromates in an inert atmosphere; (c) reduction by hydrogen of zinc dichromate leading to a mixture of zinc oxide and zinc chromite spinel which is a catalyst for methanol synthesis. The spinel has a disordered X-ray structure and has its lattice modified by interstitial zinc oxide. The experimental enthalpy change of the zinc dichromate reduction (at 320°) by hydrogen is $(-\Delta H)|_{320} = 34$ kcal/mol of H_2. By carrying out the reaction in a fixed bed differential reactor under chemical control conditions, a kinetic expression which takes into account the influence of temperature and gaseous and reactant solid molar concentrations is obtained. A reaction mechanism and a porous structure geometrical model which enables the calculation of the reactant solid surface evolution along the reaction are proposed.

Part I. Physical Chemical Study

Introduction

The preparation of a zinc oxide–chromium oxide catalyst for methanol synthesis has been the subject of many investigations (Kawamura and Irie, 1957; Irie and Shiraishi, 1959; Vlasenko, *et al.*, 1961; Zhigailo, *et al.*, 1963; Zhigailo and Shpak, 1963; Zhigailo, 1964; Kruglov and Mikhhal'ova, 1963; Kirillov, *et al.*, 1964; Opolovnikova, *et al.*, 1965; Muenzing, 1965; Uchida, *et al.*, 1965; Rozenfel'd, *et al.*, 1966; Gaidei, *et al.*, 1967; Rusov, 1968; Yakerson, *et al.*, 1969; Goroshko, *et al.*, 1969; Burzyk and Haber, 1969). However, even a slight reading of the previous references indicates that the actual knowledge of the process is rather confused because of the several reaction schemes proposed, as well as the variety of Cr–O–Zn compounds (some of them nonstoichiometric) which were postulated as intermediates in the preparation of Zn–Cr catalysts.

Though the preparation of a zinc–chromium catalyst was generally performed *in situ* in the methanol synthesis reactor, recently it has been recognized (Vlasenko, *et al.*, 1961; Rozenfel'd, *et al.*, 1966; Rusov, 1968) that random characteristics of the catalyst may be avoided by carrying out the process outside synthesis column.

In the last case, the process has three well-defined stages: (a) chromium trioxide reaction with an excess of zinc oxide and water leading to a mixture of zinc hydroxychromates ($ZnCrO_4 \cdot Zn(HO)_2$ and $ZnCrO_4 \cdot (3\text{-}4)Zn(HO)_2$); (b) heating in an inert gas (*e.g.*, air) producing the zinc hydroxychromates decomposition, giving nonidentified Zn–Cr compounds; (c) reducing these compounds by hydrogen (or methanol synthesis gas) to provide a catalyst